Optical characterization of silver-gallium: a new material for plasmonic nanostructures

A. L. Lereu,[1,2] F. Lemarchand,[2] M. Zerrad,[2] M. Yazdanpanah,[3,4] and A. Passian,[1,5,6*]
[1] *Oak Ridge National Laboratory, Oak Ridge, TN 37831-6123, USA*
[2] *Aix-Marseille Université, CNRS, Centrale Marseille, Institut Fresnel, UMR 7249, 13013 Marseille, France*
[3] *NaugaNeedles LLC, Louisville, KY, USA*
[4] *ElectroOptics Research Institute and Nanotechnology Center, University of Louisville, Louisville, KY, USA*
[5] *Department of Physics, University of Tennessee, Knoxville, TN 37996, USA and*
[6] *Department of Chemical and Biomolecular Engineering, University of Tennessee, Knoxville, TN 37996-2200, USA*
(Dated: July 21, 2014)

Silver and gallium form an alloy Ag_2Ga via a room temperature spontaneous self-assembly that exhibits remarkable mechanical and electrical properties [1] suitable for nanoscale measurements [2]. However, whether photon excitation of plasmons in this emerging nanomaterial is retained or not has not been established. Here, we present a thin film formation of Ag_2Ga via a spreading-reactive process of liquid Ga on an Ag film and a characterization of its dielectric function $\epsilon(E) = \epsilon_1(E) - i\epsilon_2(E)$ in the photon energy range 1.42 eV$\leq E <$4.2 eV. It is observed that while the plasmon damping increases, near an energy of 3.4 eV, the real part of ϵ exhibits a crossing with respect to that of Ag. Furthermore, the impact of new plasmon supporting materials [3] is discussed and in order to enable further applications in plasmonics, the possibility of photon excitation of surface plasmons in Ag_2Ga is studied.

Plasmonic and opto-mechanical systems are increasingly investigated and invoked in applications ranging from nanoscale measurement technologies such as imaging and sensing to information technologies such as quantum computers [4]. These interests have in part grown from a need for acquiring resonance and tunablity in the response of materials with useful mechanical, optical, and electronic properties. With the typical time scales in GHz range for mechanical systems and PHz range for the plasmonic systems, materials that exhibit superior rigidity, electric conductivity, and plasmonic property are of particular interest, for example in tip-enhanced microscopy and spectroscopy [5, 6]. In cases where plasmon excitation and nano-mechanical interactions (such as Van der Waals force between the probe and the sample in near field optical microscopy), may both be relevant [7–11], materials with useful mechanical as well as optical resonances can provide superior performance.

Since their discovery in 1957 [12], surface plasmons [13–15] have been extensively studied and used in numerous applications [16] such as bio and chemical sensing [17, 18], microscopy and spectroscopy [19, 20], microfluidics manipulation [21, 22] or opto-electronics [23–28]. Plasmons have also been explored as the carrier of information in nanocircuitry for example, or plasmon supporting structure as transistor replacement, i.e., plasmonster [29, 30]. Plasmon excitation in metallic nanostructures such as thin films and nanoantennas is efficiently achieved when using metals with a dielectric function possessing a large negative real part and a small imaginary part. Therefore, noble metals such as gold or silver, despite being ductile and tarnishable, are often invoked as systems to support plasmon excitation. Processes that yield mechanical and chemical enhancement while significantly preserving plasmonic properties of materials are important (Table SII compares [31] metals commonly used in nanophotonics). Both silver (Ag) and gallium (Ga) exhibit transitions that are suitable for photon excitation of plasmons [32–34]. Recently, Reifenberger et al have demonstrated, through atomic force microscopy measurements, that Ag_2Ga nanoneedles possess superior mechanical and electrical properties [35, 36] and chemical stability. To date however, to what extend the plasmonic properties are retained in Ag_2Ga has not been established. The electronic properties of noble metals such as Ag permit intraband and interband transitions and collective excitations that have made it particularly useful in many applications such as plasmonics, surface plasmon resonance (SPR) sensing, surface enhanced Raman and fluorescence spectroscopies, etc. Albeit less extensively, the band structure and optical properties of Ga have also been studied and existence of plasmon modes has been reported in the case of nanospheres [32–34, 37]. Unlike noble metals, very little attention has been given to alternative supporting platforms for plasmon excitation such as metal alloys [38–41]. West et al nicely reported on plasmon excitations using either noble metals, metal alloys, semiconductors, or graphene [3]. Naik et al presented the case of oxides and nitrides [42], while Wu et al also discussed the use of Ga nanoparticles for plasmon resonances or surface enhanced Raman spectroscopy [32]. Here, we focus on the particular case of the alloy Ag_2Ga and its optical and plasmonic properties.

A thin film of Ag_2Ga was fabricated by depositing a

*Email address: passianan@ornl.gov

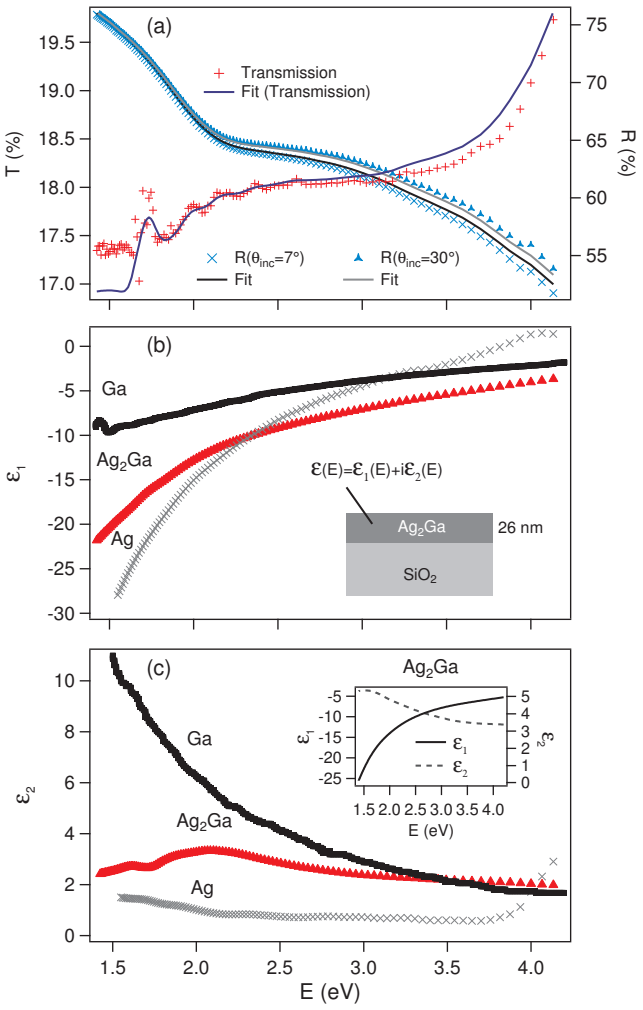

FIG. 1: Spectroscopic characterization for the determination of the dielectric function of Ag_2Ga. Reflectance and transmittance measurements (a), and the corresponding numerically obtained real (b) and imaginary (c) parts of ϵ are displayed for the geometry shown in the inset of b). Available (bulk) optical properties of both gallium [32] and silver [52] are provided for comparison. Calculated ϵ from spectroscopic ellipsometry measurements are shown in the inset of c).

Ga microdroplet on a thin film of Ag sputter-coated on a SiO_2 substrate (see Fig. S1 and Supplementary material for the reactive spreading process). We begin our study by first carrying out spectroscopic and ellipsometric measurements. We then numerically analyze the data to obtain the values of the complex dielectric function ϵ of the sample and compute the plasmon dispersion relations in the case of a substrate-supported thin film [43] corresponding to the symmetric and antisymmetric resonances of the surface charge oscillations, that is, the solutions of Eqs. S10 and S11. To better interpret the measurements, we employed electron microscopy (SEM), atomic force microscopy (AFM), X-ray photoemission spectroscopy (XPS) and profilometry to characterize the same sample. For example, from a compositional and morphological analysis with XPS and AFM, we concluded that the amount of Ga in the assembled thin film is two times that of Ag (estimated from the predominant peaks associated with the 2p3/2 and 3d5/2 orbitals of Ga and Ag, respectively, see in Table SI), with a 25 nm overall topographic variation (see the Supplementary material for the crystal formation and film characterization, Figs. S2-S4).

Spectrophotometric measurements, both in transmission and reflection, illustrated in Fig. S5a) and in Fig. S5b) respectively, were carried out in a wavelength range from 300-870 nm (1.42 to 4.2 eV) using a 1×1 mm focused beam diameter and a 2 nm resolution. A grid-less photomultiplier tube served as detector to cover the chosen spectral range, and a reflectance optics arrangement allowed translating the input mirror and polarizer and rotating the detection line to vary the incidence angle and provide control of the polarization (s and p). The transmission $T_{0,exp}$ was obtained at normal incidence under modulated light to record alternatively the baseline and the transmitted signal. The reflectance measurements included a 7° of incidence for an average polarization ($R_{7a,exp}$) and a 30° of incidence for p ($R_{30p,exp}$) and s polarization ($R_{30s,exp}$). Employing larger incident angles was not attempted to avoid elongated exposure regions that could introduce errors in the reflectance linked to inhomogeneities in the illumination region. The polarization effect was only studied in the 30° case as 7° for thin films behaves nearly as normal incidence where the polarization effect is negligible. Finally, the two optical paths (that is, the reference and the signal paths) are balanced to be equivalent, using an optical compensator, so the sample reflectance ($R = R_{sample}/R_{Baseline}$) can be directly recorded. Having obtained quantitative measurements, as shown in Fig. 1a), we now aim to extract $\epsilon(E)$ for the alloy.

Widely used physics-based models for the optical energy dispersion such as Drude, Forouhi-Bloomer (FB), and Tauc-Lorentz, taking into account the free electron gas behavior and interband transitions, satisfy the Kramers-Kronig relations. The Drude model [44], explaining the transport properties of electrons in materials, especially metals, where free electrons play a significant role in the optical properties, was improved [45] by modifying ϵ to include contributions from valence and free electrons, and phonons only by assuming a frequency-dependent relaxation energy between the plasma energy and the band gap. The Tauc-Lorentz model, which was first proposed by Jellison and Modine [46], has been frequently used for many amorphous materials but is not adapted to metallic materials. The FB model [47] is derived from the Kramers-Kronig integration and was first applied to amorphous semiconductors and dielectric materials [48]. Recently, one of us [49] reported that for metals such as ITO and Au, the best description, in the visible/infrared range, is obtained

by combining the FB multiple oscillator model and the modified Drude model by simply adding the contribution of each permittivity $\epsilon(E) = \epsilon_{FB}(E) + \epsilon_D(E)$. With eleven parameters for the description of our frequency dispersion model in conjunction with the thickness of the film, we employed a clustering global optimization (CGO) method, which minimizes the distance between the different measured and calculated spectra. Details of the optimization procedure have been reported by Gao et al. [50].

Numerical fitting (continuous blue curves in Fig. 1a)) to the spectrophotometric parameters R and T, represented in Fig. 1a), and introducing an error function (EF) (Eq. S1 in the Supplementary material) to measure the differences between the calculated and experimental R and T, yield the solutions for n and k by minimizing the EF. Here, we employed a CGO algorithm and a FB model [49], which is Kramers-Kronig consistent, to obtain the optical dispersion relations (see Eqs. S2 to S9 in the Supplementary material). The employed optimization is nontrivial due to the complex frequency dependent n and k laws. The FB model has been shown to be particularly useful for amorphous and randomly assembled morphological dissimilar materials (see SEM image in Fig. S1). CGO has been demonstrated to efficiently solve the case of thin-film problems [50] to determine the value of the dielectric function. It can be viewed as a modified form of the standard Multistart procedure [51], in which a local search is performed from several starting points distributed over the entire search domain. In cases, where a large number of starting points is used, the Multistart technique suffers the drawback of identifying the same local minimum multiple times, thereby leading to an inefficient global search. Clustering method improves the efficiency of the Multistart technique through careful selections of the points from which the local search is initiated. Using the clustering method, we obtained the n and k values by removing the aberrant solutions, i.e., solutions with large EF values or with incoherent (n, k, d) values.

Furthermore, to corroborate the n and k determination, following the R and T measurements and EF optimization, we carried out spectroscopic ellipsometry, as shown in the inset of Fig. 1c). An ellipsometer (M-2000 J. A. Wollam Co.) was configured in reflectance mode at an incident angle of 65°. After measuring the reflectance for both s and p polarizations to obtain the ellipsometry coefficients, we extracted the n and k behavior using the Lorentz oscillator model. Despite the shortcomings of the employed model for the description of metallic medium, both measurements as shown in the inset of Fig. 1c), are in relatively good agreement for the n and k laws (tabulated in the supplementary materials, Table SIII) leading to a film thickness d estimate of 26 nm. Indeed, when examining the dependencies upon the wavelength λ and d, in Fig. 2, the measured reflectance law of Fig. 1 a),

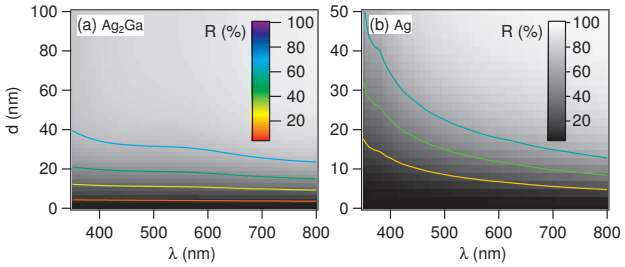

FIG. 2: Numerical fitting to the experimentally determined reflectance as a function of thickness and wavelength for a Ag_2Ga and Ag. A 26 nm thickness was obtained from the best fit to the data. Color contours are provided for clarity.

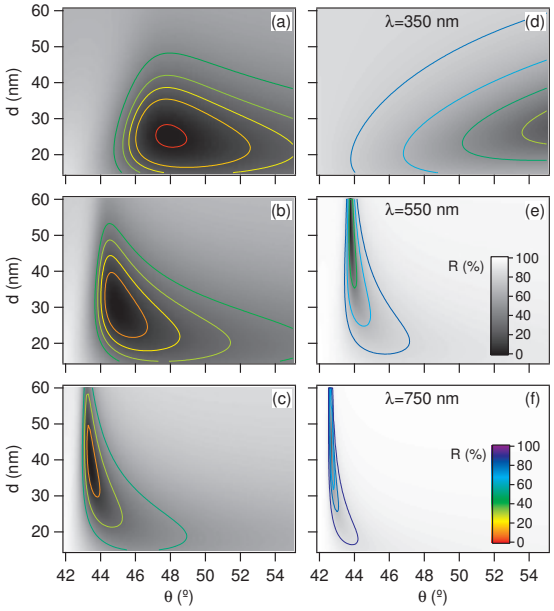

FIG. 3: Predicted reflectance R as functions of film thickness d and angle of incidence θ for a film of Ag_2Ga (a)-(c) and silver (d)-(f) at three different wavelengths λ. Color contours are provided for clarity.

varying between 55% at 300 nm up to 75% at 870 nm, corresponds to a Ag_2Ga film of 26 nm. When comparing the determined obtained permittivity laws with those of Ag, in Fig. 1b) for ϵ_1 and Fig. 1c) for ϵ_2, one can see that ϵ_2 is globally higher for Ag_2Ga than for Ag, while a common point for ϵ_1 appears around λ=550 nm. Both at and on either side of this spectral position, we examine the plasmonic response of a thin Ag_2Ga film, specifically at wavelengths λ=350 nm, 550 nm, and 750 nm, as shown in Fig. 3.

In Fig. 3, the reflectance is studied and compared to that of a corresponding Ag film as functions of the film thickness d and the incident angle θ for the three wavelengths above. As guided by the scale bars, while for the shorter wavelength, the contours express a more pro-

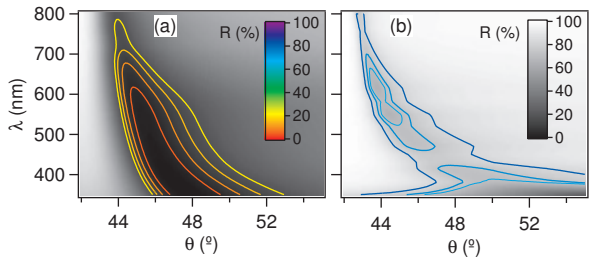

FIG. 4: Expected reflection as a function of wavelength and incident angle θ for a 26 nm Ag_2Ga film (a) and Ag film (b). Color contours are provided for clarity.

nounced plasmon resonance in the considered parameter ranges for Ag_2Ga, the trend is somewhat reversed for the longer wavelengths. Indeed, for larger wavelengths, the reflectance approaches zero in the case of Ag_2Ga films but the resulting resonance peak becomes increasingly broad. We also note that, similar to the cases of Au and Ag, no plasmon resonances occur under excitation with s polarized light. To further illustrate the plasmon resonance in the measured Ag_2Ga film, the specific thickness $d = 26$ nm was considered for the absorption properties as a function of θ and λ. As Fig. 4 shows, the structure supports surface plasmon resonances over the full spectral range with peak widths in the range from 2° down to fractions of a degree. In the case of a thin metal film deposited on an optically conductive dielectric medium, the archetype system for many plasmon investigations including the SPR, collective oscillations can occur symmetrically or anti symmetrically on the two surfaces of the film. These properties can be captured in the plasmon dispersion relations for the metal coated dielectric system, as shown in Fig. 5 (See Eqs. S10 and S11), where comparison is made between the resonant excitations in Ag versus Ag_2Ga films for various film thicknesses given by the color scale (from 15 up to 100 nm). The insets give the resulting reflectance curves for the three identified wavelengths for 26 nm thick metal films associated with a quartz prism and surrounded with Air.

In conclusion, the alloy formation Ag_2Ga, here controlled to fabricate a 26 nm thin film, was established to yield useful plasmonic properties. The slope of the measured ϵ_1 for this nanomaterial suggests that its plasma frequency lies below that of Ga at $\omega_p^{Ga} \approx 21$ eV [53] and above that of Ag at $\omega_p^{Ag} \approx 3.8$ eV [52]. The first time experimental determination of the dielectric function of Ag_2Ga opens up new opportunities in opto-mechanics and plasmonics where specific mechanical as well as optical properties are required. While the optical properties retain some similarity with Ag, the plasmon excitation in Ag_2Ga thin films comparatively seems to exhibit an enhancement in the shorter wavelength part of the spectrum and a deterioration in longer wavelength part of

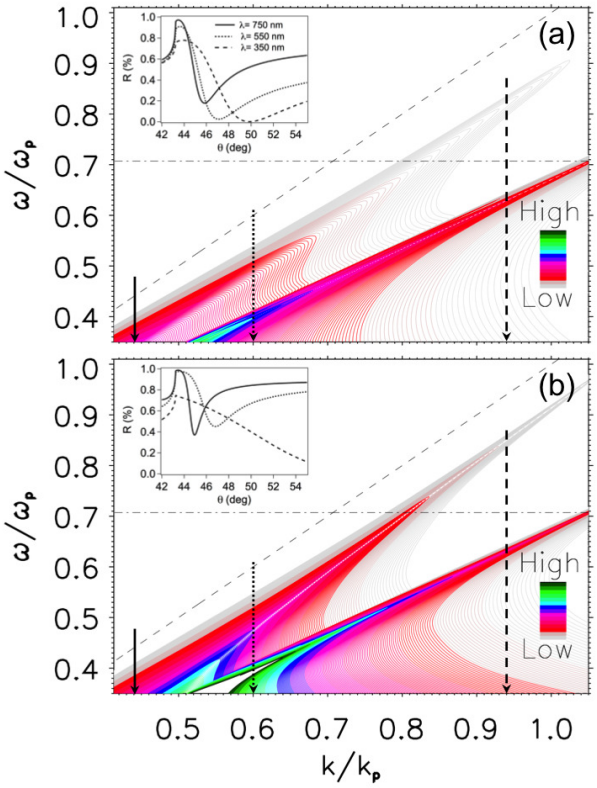

FIG. 5: Plasmon dispersion relations for Ag_2Ga (a) and Ag (b) films of 26 nm on SiO_2. Overall, two branches (due to the presence of two interfaces, that is, alloy-vacuum and alloy-SiO_2 interfaces are visible. The appearance of the higher energy band corresponding to the antisymmetric surface charge density oscillations, while more pronounced in the case of Ag can vary slightly depending upon the numerical processing. The insets provide the expected angular dependence of the plasmon resonances.

the visible spectrum. The latter appears in the form of a broadening of the resonances due to damping of the plasmons. The rigidity of Ga is observed to be advantageous at the price of the elevated plasmon damping when compared to silver. The obtained numerical data (summarized for convenience in Table SIII) can provide input for numerical and computational techniques such as the finite difference time domain (FDTD) and finite elements (FE), where absorption spectra and field distribution can be calculated for a variety of nanoparticles, provided their dielectric function can be sampled or represented analytically in form of Drude, Drude-Lorentz, or other appropriate models. In addition to useful mechanical and thermal properties, Ag_2Ga possesses attractive optical properties in near UV-visible spectral range suggesting potential use in investigations involving surface modes and plasmon excitation such as surface- and tip-enhanced spectroscopies.

Acknowledgments

This research was supported in part by the laboratory directed research and development fund at Oak Ridge National Laboratory (ORNL), and in part by Nauga-Needles LLC, and the Centre National de la Recherche Scientifique (CNRS). The authors would like to thank CNRS researchers Drs. A. Charrier, J-Y. Hoarau, and A. Ranguis for their help with XPS and AFM characterization. ORNL is managed by UT-Battelle, LLC, for the US DOE under contract DE-AC05-00OR22725.

[1] M. M. Yazdanpanah, S. A. Harfenist, A. Safir and R. W. Cohn, J. Appl. Phys. **98**, 073510 (2005).
[2] L. B. Biedermann *et al.*, Nanotechnology **21**, 305701 (2010).
[3] P. R. West, S. Ishii, G. V. Naik, N. K. Emani, V. M. Shalaev, and A. Boltasseva, Laser photonics Rev. **4**, 795 (2010).
[4] F. Marquardt, Optomechanics, Physics 2, 40 (2009).
[5] B. Pettinger, P. Schambach, C. J. Villagomez, and N. Scott, Annual Review of Physical Chemistry **63**, 379 (2012).
[6] T. Schmid, L. Opilik, C. Blum and R. Zenobi, Angewandte Chemie Int. Ed. **52**, 5940 (2013).
[7] Pohl, D.W. and Novotny, L., J. Vac. Sci. Technol., B **12**, 1441 (1994).
[8] van Hulst, N.F. and Moers, M.H.P. IEEE Eng. Med. Biol. **15**, 51 (1996).
[9] Dunn, R.C. Chem. Rev. **99**, 2891 (1999).
[10] Hecht, B., Sick, B., Wild, U.P., Deckert, V., Zenobi, R., Martin, O.J.F. and Pohl, D.W. J. Chem. Phys., **112**, 7761 (2000).
[11] De Serio, M., Zenobi, R. and Deckert, V., Trends Anal. Chem. **22**, 71 (2003).
[12] R. H. Ritchie, Phys. Rev. **106**, 874 (1957).
[13] H. Raether, Surface Plasmons on Smooth and Rough Surfaces and on Gratings, New York: Springer-Verlag (1988).
[14] S. Bozhevolnyi, and F. Garcia-Vidal, New J. Phys. **10**, 105001 (2008).
[15] S. Hayashi, and T. Okamoto, J. Phys. D: Appl. Phys. **45**, 433001 (2012).
[16] J. Heber, Nature **461**, 720 (2009).
[17] J. N. Anker, W. P. Hall, O. Lyandres, N. C. Shah, J. Zhao and R. P. Van Duyne, Nature Materials **7**, 442 (2008).
[18] A. G. Brolo, Nature photonics **6**, 709 (2012).
[19] S. Kawata, Y. Inouye and Prabhat Verma, Nature photonics **3**, 388 (2009).
[20] F. De Angelis, F. Gentile, F. Mecarini, et al Nature photonics **5**, 682 (2011).
[21] A. Passian, S. Zahrai, A. L. Lereu, R. H. Farahi, T. L. Ferrell, and T. Thundat, Phys. Rev. E 73, 066311 (2006).
[22] R. H. Farahi, A. Passian, S. Zahrai, A. L. Lereu, T. L. Ferrell, and T. Thundat, Ultramicroscopy 106, 815 (2006).
[23] A. Passian, A. L. Lereu, E. T. Arakawa, R. H. Ritchie, T. Thundat, and T. L. Ferrell, Appl. Phys. Lett. **85**, 2703 (2004).
[24] A. Passian, A. L. Lereu, E. T. Arakawa, A. Wig, T. Thundat, and T. L. Ferrell, Opt. Lett. **30**, 41 (2005).
[25] A. L. Lereu, A. Passian, J-P. Goudonnet, T. Thundat, and T. L. Ferrell, Appl. Phys. Lett. **86**, 154101 (2005).
[26] A. L. Lereu, Nature Photonics **1**, 368 (July 2007).
[27] E. Ozbay, Science **311**, 189 (2006).
[28] R. Zia, J. A. Schuller, A. Chandran, and M. L. Brongersma, Materials today **9**, 20 (2006).
[29] A. E. Chang, A. S. Sorensen, E. A. Demler, and M. D. Lukin, Nature materials **3**, 807 (2007).
[30] H. A. Atwater, Scientific American, 56 (2007).
[31] http://www.periodni.com
[32] P. C. Wu, C. G. Khoury, T-H. Kim, Y. Yang, M. Losurdo, G. V. Bianco, T. Vo-dinh, A. S. Brown, and H. O. Everitt, J. Am. Chem. Soc. **131**, 12032 (2009).
[33] O. Hunderi and R. Ryberg J. Phys. F: Metal Phys. **4** 2084 (1974).
[34] G. Jezequel, J. C. Lemonnier and J. Thomas J. Phys. F: Metal Phys. **7** 1613 (1977).
[35] R. G. Reifenberger, R. A. Raman, L. Biedermann, and M. M. Yazdanpanah, Ultra-soft atomic force microscope (USAFLM), (2009).
[36] M. M. Yazdanpanah, PhD Dissertation University of Louisville (2006).
[37] J.A. Creighton R. Withnall, Chemical Physics Letters **326** 311 (2000).
[38] B. M. Hartley, and J. B. Swan, Aust. J. Phys. **23**, 655 (1970).
[39] S. A. Abo-Namous P. T. Andrews and C. E. Johnson, J. Phys. F: Met. Phys. **9**, 61 (1979).
[40] A. Tadjeddine, A. F. Benhabib, A. Zeghib and J. Le Bas, J. Phys. France **48**, 1715 (1987).
[41] D. Y. Lei, J. Li, and H. C. Ong, Appl. Phys Lett. **91**, 021112 (2007).
[42] G. V. Naik, J. Kim, A. Boltasseva, Opt. Mater. Express **1**, 1090 (2011).
[43] Z. Kretschmann, Z. Phys. **241**, 313 (1971).
[44] P. Drude, Annalen der Physik **306**, 566 (1900).
[45] I. Hamberg and C. G. Granqvist, J. Appl. Phys. **60**, R123 (1986).
[46] G. E. Jellison, Jr., and F. A. Modine, Appl. Phys. Lett. **69**, 371, 2137 (1996).
[47] A. R. Forouhi and I. Bloomer, Phys. Rev. B **38**, 1865 (1988).
[48] A. R. Forouhi and I. Bloomer, Phys. Rev. B **34**, 7018 (1986).
[49] L. Gao, F. Lemarchand and M. Lequime, Thin Solid Films **520**, 501 (2011).
[50] L. Gao, F. Lemarchand and M. Lequime, Appl. Phys. A **108**, 877 (2012).
[51] A. H. G. Rinnooy Kan, and G. T. Timmer, Mathematical Programming **39**, 57 (1987).
[52] E. D. Palik, Handbook of Optical Constants of Solids Academic Press, Orlando, (1985).
[53] I. N. Shklyarevskiœ, Yu. Yu. Bondarenko, and N. A. Makarovskiœ, Optics and Spectroscopy **88**, 547 (2000). Translated from Optika